Wideband four-level transmission gratings with flattened spectral efficiency

Juha Pietarinen, Tuomas Vallius, and Jari Turunen

University of Joensuu, Department of Physics,
B.O. Box 111, FI-80101 Joensuu, Finland
Juha.Pietarinen@joensuu.fi

Abstract: Four-level transmission-type surface relief grating profiles with nearly flat efficiency over a spectral octave are designed by rigorous electromagnetic diffraction theory. Parametric optimization of the relief depths and transition points of the profile steps of these leads to efficiencies in the range 50–60% over the entire octave if the ratio of the grating period and the mean spectral wavelength is greater than ~ 3.

OCIS codes: (050.1970) Diffractive optics; (050.1960) Diffraction theory;

References and links

1. B. Braam, J. Okkonen, M. Aikio, K. Makisara, J. Bolton, "Design and first test results of the Finnish airborne imaging spectrometer for different applications, AISA", in *Imaging Spectrometry of the Terrestial Environment*, G. Vane, ed., Proc. SPIE **1937,** 142–151 (1993).
2. S. H. Kong, D. D. L. Wijngaards, and R. F. Wolffenbuttel, "Infrared micro-spectrometer based on diffraction gratings," Sensors and Actuators A **92,** 88–95 (2001).
3. F. Salem and M. Kafatos, "Hyperspectral image analysis for oil spilling mitigation,", in *Proceedings of 22nd Asian Conference on Remote Sensing*, (CRISP, Singapore, 2001) pp. 748–753.
4. E. Herrala and J. Okkonen, "Imaging spectrograph and camera solutions for industrial applications," Int. J. Pattern Recogn. Artif. Intellig. **10**, 43–54 (1996).
5. R. O. Green, "Spectral calibration requirement for Earth-looking imaging spectrometers in the solar-reflected spectrum," Appl. Opt. **37,** 683–690 (1998).
6. P. Mouroulis, D. W. Wilson, P. D. Maker, and R. E. Muller, "Convex grating types for concentric imaging spectrometers," Appl. Opt. **37,** 7200–7208 (1998).
7. P. Mouroulis, "Spectral and spatial uniformity in pushbroom imaging spectrometers," in *Imaging Spectrometry V*, J. B. Rafert, W. J. Slough, C. A. Rohde, A. Pilant, L. J. Otten, A. D. Meigs, A. Jones, and E. W. Butler, eds. Proc. SPIE **3753,** 133–141 (1999).
8. T. Hyvarinen, E. Herrala, and A. Dall'Ava, "Direct sight imaging spectrograph: a unique add-on component brings spectral imaging to industrial applications," in *Digital Solid State Cameras: Design and Applications*, G. M. Williams, ed., Proc. SPIE **3302,** 165–175 (1998).
9. E. Herrala, J. Okkonen, T. Hyvarinen, M. Aikio, and J. Lammasniemi, "Imaging spectrometer for process industry applications," in *Optical Measurements and Sensors for the Process Industries*, C. Gorecki and R. W. Preater, eds., Proc. SPIE **2248,** 33–40 (1994).
10. D. E. Battey and J. B. Slater, "Compact holographic imaging spectrograph for process control applications," in *Optical Methods for Chemical Process Control*, S. Farquharson, ed., Proc. SPIE **2069,** 60–64 (1997).
11. E. Cianci, V. Foglietti, F. Vitali, D. Lorenzetti, A. Notargiacomo, and E. Giovine "Micromachined silicon grisms: high resolution spectroscopy in the near infrared," Microelectron. Eng. **53**, 543–546 (2000).
12. P. Laakkonen, M. Kuittinen, J. Simonen, and J. Turunen, "Electron-beam-fabricated asymmetric transmission gratings for microspectrometry," Appl. Opt. **39**, 3187–3191 (2000).
13. H. P. Herzig, ed., *Micro-optics: Elements, Systems and Applications* (Taylor & Francis, London, 1997).
14. J. Turunen and F. Wyrowski, eds., *Diffractive Optics for Industrial and Commercial Applications* (Wiley-VCH, Berlin, 1997).
15. M. C. Hutley, *Diffraction Gratings* (Academic Press, Orlando, 1982).
16. R. Petit, ed., *Electromagnetic Theory of Gratings* (Springer, Berlin, 1980).

#68204 - $15.00 USD Received 17 February 2006; revised 21 March 2006; accepted 21 March 2006

17. J. Turunen, M. Kuittinen, and F. Wyrowski, "Diffractive optics: electromagnetic approach," in *Progress in Optics*, E. Wolf, ed., vol. XL, chap. V (Elsevier, Amsterdam, 2000).
18. L. Li, "Use of Fourier series in the analysis of discontinuous periodic structures," J. Opt. Soc. Am. A **13**, 1870–1876 (1996).
19. E. Noponen and J. Turunen, "Binary high-frequency-carrier diffractive optical elements: electromagnetic theory" J. Opt. Soc. Am. A **11,** 1097–1109 (1994).
20. E. Noponen, A. Vasara, and J. Turunen, "Parametric optimization of multilevel diffractive optical elements by electromagnetic theory," Appl. Opt. **31**, 5910–5912 (1992).
21. E. Noponen, J. Turunen, and A. Vasara, "Electromagnetic theory and design of diffractive-lens arrays," J. Opt. Soc. Am. A **10,** 434–443 (1993).
22. K. Blomstedt, E. Noponen, and J. Turunen, "Surface-profile optimization of diffractive imaging lenses," J. Opt. Soc. Am. A **18,** 521–525 (2001).
23. C. David "Fabrication of stair-case profiles with high aspect ratios for blazed diffractive optical elements,"Microelectron. Eng. **53**, 677–680 (2000).
24. K. Jefimovs, Ph.D. Thesis (University of Joensuu, 2003).

1. Introduction

There is increasing demand for compact and low-cost spectrometers in, e.g., environmental, biological, and chemical sensing, and in process analysis [1–4]. High spectral resolution is not necessarily required — sometimes it is sufficient to resolve only tens of adjacent spectral channels or to monitor just a few characteristic spectral features — but the dispersion must typically be moderately high to achieve a compact design. The spectral range should often be wide (perhaps extending over an octave), and reasonably uniform spectral (and spatial) response is much preferred, particularly in pushbroom imaging spectrometers, to obtain fast and accurate spectral measurements [5–8].

There are several good reasons to employ transmission gratings rather than reflection gratings in compact imaging spectrometers [9, 10]. Transmission gratings allow the construction of compact, low-cost, low-f-number instruments [10] and even direct-vision GRISM [11] based constructions [9]. However, the optimization of transmission grating profiles for high and uniform efficiency over a wide spectral range has received only limited attention [6, 8, 12]. Such designs, with a flat octave-wide spectral response, are provided here. Since the spectrum is usually converted to digital form, variations in the spectral response diminish the accuracy of the analysis. Hence responses independent of the wavelength are of interest e.g., in imaging spectrometers.

To obtain dispersion values of interest in compact spectrometers, the ratio of the grating period d and the center wavelength $\bar{\lambda}$ of the spectral response is chosen to be 3–10. Four-level profile shapes considered because they have a sufficient number of degrees of freedom for optimization and because they are compatible with an accurate microlithographic fabrication process.

The paper is organized as follows. In sect. 2 we introduce the type of profile to be considered, including the free parameters to be optimized, and justify this choice. The design method based on parametric optimization and rigorous electromagnetic grating theory is presented in sect. 3 along with the merit functions used in the optimization. In sect. 4 we provide specific design results for selected values of the ratio $d/\bar{\lambda}$. Finally, conclusions are drawn in sect. 5.

2. Choice of grating profile type

During the past two decades great advances in diffractive optics [13, 14] have been achieved by applying techniques such as electron beam lithography, thin-film deposition, and reactive ion etching to fabricate microrelief profile in dielectric substrates. In grating fabrication these techniques facilitate far greater control over the profile shape than the more traditional ruling and holographic exposure [15] methods do; however, they are not inherently ideal for high-

#68204 - $15.00 USD Received 17 February 2006; revised 21 March 2006; accepted 21 March 2006

resolution spectroscopic applications because of ghosts introduced by stitching of the writing fields of electron beam exposure systems and the difficulty in generating large gratings on curved substrates. Fortunately these are not primary issues in our applications, and therefore we use the freedoms in profile shape allowed by lithographic fabrication. On the other hand, the relatively high dispersion required to achieve compact devices requires d/λ ratios of the order of 3–10. One then speaks of resonance-domain gratings, which must be analyzed by rigorous electromagnetic theory [16, 17]. We use the Fourier Modal Method (FMM) with fast factorization [18] in the design process.

The choice of the grating profile type to be considered is a critical issue. On one hand it should be realizable at high precision because profile-shape errors of just tens of nanometers degrade the performance substantially in the resonance domain. On the other hand, a sufficient number of parameters should be available for successful optimization. To put the latter aspect into perspective we note that high efficiencies (above 96% for unpolarized light) can be achieved even with binary profiles if Bragg incidence is used and the profile depth as well as the fill factor are optimized [19]. However, because of the Bragg selectivity, this is possible only over a severely limited spectral range. Similarly, triangular profiles can yield high efficiencies if the profile height (and possibly also the angle of incidence) is optimized; however, even if a 'split' triangle is used to provide an additional degree of freedom [6], adequate spectral flattening over a wide spectral range can not be achieved.

Returning to the issue of feasibility of precise lithographic fabrication, we refer to a double-exposure electron beam lithographic process introduced by David [23], which is available to us in a somewhat modified form [24]. This process is capable of generating four-level profiles of the type shown in Fig. 1 with nearly vertical sidewalls, sharp and exactly placed transitions, and highly precise depth levels. The free parameters for optimization are now the transition point locations x_j and the profile depths z_j, with $j = 1,2,3$, and also the angle of incidence θ if so desired. This choice of general profile shape is motivated not only by feasibility of fabrication, but also by our experience in designing diffractive elements with spatially variable local period for monochromatic light of wavelength λ_0 [20–22]: it was observed that not much can be gained by using more than four levels if the transition points x_j are optimized. The results of Refs. [20–22] are not applicable here since we are not optimizing the profile for one value of the ratio d/λ_0 at a time, but for an extended range $\Delta\lambda$ with a fixed ratio d/λ.

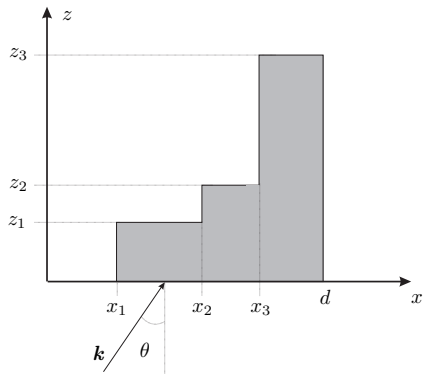

Fig. 1. The type of transmission-grating profile considered in this paper, with illustration of the free optimization parameters x_j, z_j ($j = 1,2,3$), and θ.

#68204 - $15.00 USD Received 17 February 2006; revised 21 March 2006; accepted 21 March 2006

3. Design method

Parametric optimization with the Nelder-Mead simplex method is employed to search for optimum values of x_j and z_j. In order to evaluate the merit of each configuration, FMM is used to calculate the spectral efficiency curves $\eta_{\mathrm{TE}}(\lambda)$ and $\eta_{\mathrm{TM}}(\lambda)$ of diffraction order -1 at N sample values λ_n of the wavelength λ within the chosen spectral interval (the subscripts TE and TM denote TE and TM polarization, respectively). The number diffraction orders M used during optimization was typically $M \sim 15$ in TE polarization and $M \sim 20$ in TM polarization to ensure a satisfactory trade-off between convergence and computational cost (which increases $\propto M^3$ in FMM), and the final results were verified using a larger number of orders. The most natural starting point of optimization is a regular four-level profile with equally spaced values of x_j and z_j, but since the Nelder-Mead algorithm converges to the nearest local minimum several initial distributions with modified values of x_j and z_j may have to be tried to find an acceptable solution of this nonlinear optimization problem.

In the first stage of the design procedure we use a least-squares-type merit function of the form

$$\mathrm{MF} = \sum_{n=1}^{N} \left[\frac{1}{2}\eta_{\mathrm{TE}}(\lambda_n) + \frac{1}{2}\eta_{\mathrm{TM}}(\lambda_n) - \bar{\eta} \right]^2 \tag{1}$$

where

$$\bar{\eta} = \frac{1}{2N} \sum_{n=1}^{N} \left[\eta_{\mathrm{TE}}(\lambda_n) + \eta_{\mathrm{TM}}(\lambda_n) \right] \tag{2}$$

is the mean value of the efficiencies at $\lambda = \lambda_n$ for unpolarized light. The mean value $\bar{\eta}$ is allowed to evolve freely during this optimization stage, i.e., no attempt is yet made to ensure a high overall efficiency. As a result a flat response is obtained fairly rapidly but $\bar{\eta}$ typically reduces to values of the order of 20%. The aim of the second optimization stage is the improve the efficiency without sacrificing the achieved uniformity of the spectral response. To this end one can, for example, replace $\bar{\eta}$ with some goal value η_{g}, which is gradually raised during optimization until no further improvement is possible without a substantial increase of MF. Alternatively, some other form of merit function can be used during the second stage, as long as it is designed to push up the value of $\bar{\eta}$ one way or the other.

4. Results

Keeping in mind the dispersion requirements in our applications, we are primarily interested in values of $d/\bar{\lambda}$ in the range 3–10. We choose a spectral range extending over a full octave in the near-infrared region, namely $1\ \mu\mathrm{m} < \lambda < 2\ \mu\mathrm{m}$, and provide specific designs for $d = 5\ \mu$ and $d = 11\ \mu\mathrm{m}$. This spectral range is of interest in numerous applications of pushbroom spectrometers, but designs can easily be obtained for other values of $\bar{\lambda}$ by appropriate scaling and using correct values for the (wavelength-dependent) refractive index of the substrate (incidence from an SiO_2 substrate to air is assumed here, and the conditions $z_3 > z_2 > z_1$ are maintained).

The main results are collected in Figs. 2–4 and Tables 1 and 2. In addition to spectral flattening (green lines in Fig. 2), we also optimized the profiles for maximum efficiency using $\bar{\eta}$ defined by Eq. (2) as a merit function (red lines in Fig. 2). This is seen to improve the efficiency substantially if $d = 5\ \mu\mathrm{m}$, but not when $d = 11\ \mu\mathrm{m}$. In both cases the flattened efficiency curves are rather similar for unpolarized light, with the efficiency varying in the range 52–60%. Even though the optimization result in the maximum-efficiency case at $d = 11\ \mu\mathrm{m}$ is nearly the same as the non-optimized result, the transition points are shifted noticeably, and flattening of the efficiency curve changes especially the last step height. With $d = 5\ \mu\mathrm{m}$ the lateral and vertical shifts of the parameters are even more remarkable. Finally, fabrication errors of ± 20 nm in x_j or z_j lead to efficiency degradation of the order of 2%.

#68204 - $15.00 USD Received 17 February 2006; revised 21 March 2006; accepted 21 March 2006

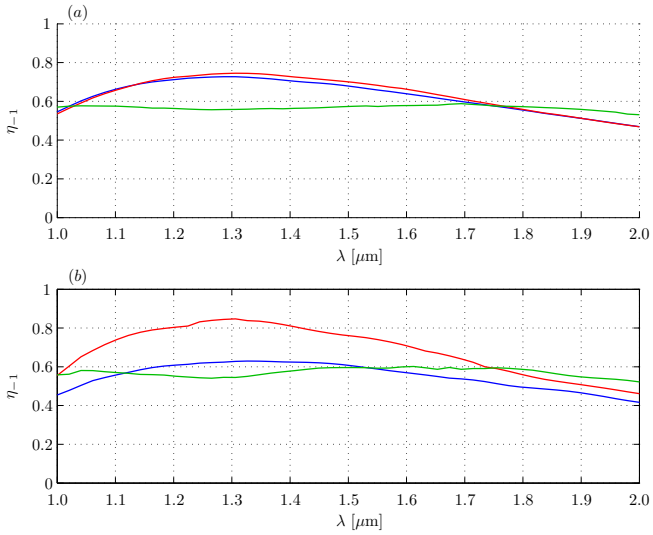

Fig. 2. Spectral efficiency curves of order -1 for unpolarized light with (a) $d = 11\mu$m and (b) $d = 5\ \mu$m. Blue: regular staircase profile. Red: optimized overall efficiency. Green: flattened efficiency.

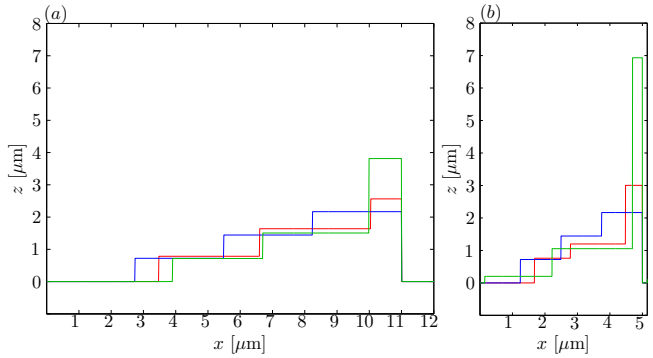

Fig. 3. Grating profiles with (a) $d = 11\mu$m and (b) $d = 5\ \mu$m. Blue: regular staircase profile. Red: profiles with optimized overall efficiency. Green: profiles with flattened efficiency.

Table 1. Quantitative characterization of the grating profiles illustrated in Fig. 3.

d [μm]	Design	$[x_1/d, x_2/d, x_3/d]$	$[z_1, z_2, z_3]$ [μm]	θ [°]
11	regular profile	0.250,0.500,0.750	0.722,1.444,2.166	0
11	maximum efficiency	0.317,0.601,0.914	0.784,1.637,2.563	0
11	flattened efficiency	0.356,0.610,0.909	0.714,1.507,3.815	-9.9
5	regular profile	0.250,0.500,0.750	0.722,1.444,2.166	0
5	maximum efficiency	0.337,0.558,0.897	0.796,1.200,3.003	1.3
5	flattened efficiency	0.031,0.445,0.940	0.203,1.055,6.932	0

It is remarkable that the efficiency curves in the two cases, $d = 11\ \mu$m and $d = 5\ \mu$m, are so similar. However, this is true for unpolarized light only, as illustrated in Fig. 4. Here the

#68204 - $15.00 USD Received 17 February 2006; revised 21 March 2006; accepted 21 March 2006

efficiency curves are plotted separately for TE and TM polarized incident fields, and the average curve for unpolarized light (already shown in Fig. 3) is given for comparison. Clearly, if $d = 11$ μm, the operation of the grating is nearly polarization-independent, which is understandable because the grating period-to-wavelength ratio approaches the 'scalar regime' $d/\lambda \gg 1$. Even though the structure is nearly polarization independent, analysis with scalar theory yields response strongly dependent on the wavelength thus proving that the scalar theory is not valid yet. However, if $d = 5$ μm, the response is strongly polarization-sensitive (as is typical in the resonance domain) but the TE and TM contributions compensate for each other.

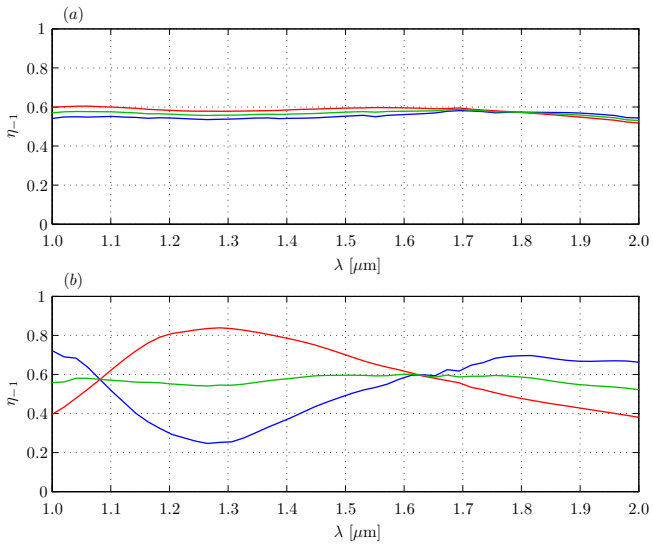

Fig. 4. Polarization sensitivity of flattened diffraction efficiency curves with (a) $d = 11\mu$m and (b) $d = 5$ μm. Blue: TE polarization. Red: TM polarization. Green: unpolarized light.

The results have been presented explicitly for only two values of d, but these are representative in the entire range $d\lambda > 3$. If $d > 11$ μm, the optimized values of x_j/d and z_j given in Table 1 for the flattened response with $d = 11$ μm still give a rather good results. If the period is reduced from 11 μm to 5 μm, the values of the parameters required for flat response change, the efficiency curve for unpolarized light remain rather unchanged, but the polarization sensitivity increases. The tabulated results for $d = 5$ μm or $d = 11$ μm can be used as a starting point for optimization at nearby values of the period.

5. Conclusions

We have used parametric optimization and rigorous electromagnetic grating theory to design multilevel transmission-grating profiles with thus-far unparalleled spectral flatness over a one-octave range. The profile type was chosen to have the degrees of freedom offered by a specific lithographic fabrication process. When used in optical configurations that also provide sufficient spatial uniformity in, e.g., pushbroom imaging spectrometers, these grating profiles are ideal for numerous spectral sensing and monitoring applications.

Acknowledgments

The work of T. Vallius and J. Turunen was supprted by the Academy of Finland (projects 106410 and 207523). The European Union Network of Excellence on Micro-Optics (NEMO, www.micro-optics.org) and discussions with Pasi Laakkonen are acknowledged.

#68204 - $15.00 USD Received 17 February 2006; revised 21 March 2006; accepted 21 March 2006